Available online at www.sciencedirect.com

SCIENCE DIRECT

Diamond & Related Materials 14 (2005) 994–999

DIAMOND AND RELATED MATERIALS

www.elsevier.com/locate/diamond

Protective diamond-like carbon coatings for future optical storage disks

F. Piazza[a,*], D. Grambole[b], D. Schneider[c], C. Casiraghi[a], A.C. Ferrari[a], J. Robertson[a]

[a]*Department of Engineering, University of Cambridge, Cambridge, CB2 1PZ, UK*
[b]*Forschungszentrum Rossendorf, Dresden, Germany*
[c]*Fraunhofer Institute for Material and Beam Technology IWS, Dresden, Germany*

Available online 18 January 2005

Abstract

Diamond-like carbon (DLC) is a promising protective coating for future optical storage technologies. The requirements place conflicting constraints on the nature of the DLC. It must be transparent at 400 nm, hard and wear-resistant, uniform, pinhole-free, have a low stress and be deposited at high rate without a high heat load on a plastic substrate. In order to optimise the films under these constraints, we have studied in detail the band gap, stress, density and Young's modulus of hydrogenated amorphous carbon (a-C:H) films deposited by plasma enhanced chemical vapour deposition using a large area electron cyclotron wave resonance source of 14 in. diameter and a variety of hydrocarbon gas sources. We have been able to produce wear-resistant carbon coatings with a high transparency at 400 nm without damaging the plastic disks. We also show that for these films the refractive index can be used as a rapid empirical means of property correlation.

Keywords: Diamond like carbon; Hydrogenated amorphous carbon; PECVD; Protective coatings; Characterisation

1. Introduction

The target of the new generation of ultra-high density optical storage devices is to reach 100 GB for a 12-cm-diameter compact disk (CD) [1]. One approach to achieve this objective is to use the flying head technology, which is used in magnetic hard disk drives (HDD). The key feature of the new generation of optical storage devices will be a very small free working separation between the objective lens or a magnetic modulation device and the storage disk. A head to disk spacing of ~1–2 μm is required for a slider flying in the optical far-field detection [2,3]. A head to disk spacing of only ~50 nm is required in the optical near field range approach, with the slider carrying a solid immersion lens as in Fig. 1. The straightforward way to achieve such a small separation is to mount the lens on a slider, which flies above the spinning disk at a constant height on a hydrodynamic air bearing, without needing a complicated servo system [4] (Fig. 1). In those conditions, a wear-resistant layer is needed to protect the disk and slider from head crashes. Magnetic hard disks use amorphous carbon as a protective coating [5–8]. This is used because it makes extremely smooth, continuous and chemically inert films, with a surface roughness well below 1 nm [9]. They provide protection against corrosion, mechanical wear and damage during head crashes. Their surfaces are compatible with the lubricant. However, carbon coatings for magnetic storage disks do not need to transmit light. Also, magnetic disks are on rigid alumina substrates whereas optical disks are much softer plastic substrates, which bend more easily under stress, and in some technologies, strain could affect the magneto-optical performance of the storage medium.

In the case of flyable high-density optical storage devices, the requirements place strong but conflicting constraints on the nature of the carbon film. It must be transparent at the recording wavelength (400 nm), hard and wear-resistant. It must have a low stress of well under 250 MPa so as not to bend the plastic substrate and be deposited at high rate without a high heat load onto such a heat-sensitive substrate. Generally, hydrogenated amorphous carbon (a-C:H) coatings of high hardness do not have a large optical gap, and they also suffer from a high compressive stress. The band gap is maximum, and the stress is minimum for soft films [10]. It is

* Corresponding author.
E-mail address: fabrice@adam.uprr.pr (F. Piazza).

0925-9635/$ - see front matter © 2004 Elsevier B.V. All rights reserved.
doi:10.1016/j.diamond.2004.12.028

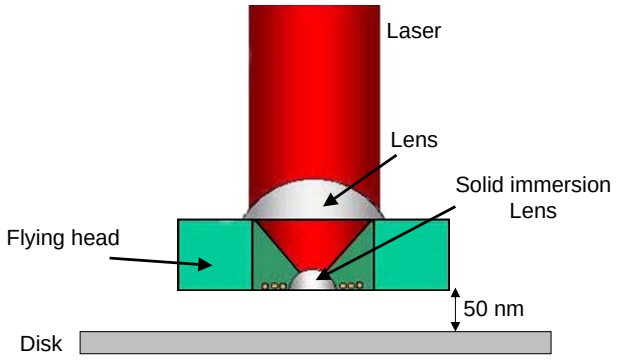

Fig. 1. Schematic of next generation high-density optical storage device with a slider immersion lens slider.

possible to obtain harder films by increasing the C–C sp^3 fraction. The hardness has been found to increase with the sp^3 fraction [11,12]. Even though high stress is not necessarily the cause of the C–C sp^3 bonding [13], deposition conditions which produce a high sp^3 fraction generally also tend to give a high stress [10,12,13]. Hence, it could be difficult to prepare a transparent, hard, stress-free film.

To obtain a gap of around 3 eV is a significant challenge in DLC. It is known that the π states introduced by the sp^2-carbon determine the gap, but the relationship between the structure and gap is not unique. The optical gap generally decreases monotonically with the increase of the sp^2 fraction in as-deposited a-C:H films [10,14]. However, the gap actually depends on the precise arrangement of the sp^2 sites, not just the sp^2 fraction [10,14,15]. The clustering of the sp^2 phase, for a given sp^3 content, reduces the band gap. In some a-C:H films the gap decreases with the increase of the stress and sp^3 fraction [16]. One of the few methods to increase the band gap of a-C:H is to introduce more hydrogen during deposition, for example, by using a hydrogen-rich precursor gas such as methane [12], which tends to reduce sp^2 cluster sizes. However, this is at a cost of a reduction in mechanical properties.

In addition, the energy flux during film growth onto plastic substrates of low thermal conductivity must be controlled, to prevent over-heating and preserve the substrate integrity. This is a significant problem as the diamond-like character increases with the ion flux ratio for a given ion energy [16,17].

The technological requirement is to produce uniform coatings over 12 cm without pinholes. We therefore choose to use plasma enhanced chemical vapour deposition (PECVD). Sputtering could also be used to deposit over large areas, but the energy deposition is likely to result in too high heat load on the substrate.

We choose to use a large area 14.2-in.-diameter Electron Cyclotron Wave Resonance (ECWR) plasma source to deposit the a-C:H films. This is because it is a compact source able to deposit over large areas with ±5% uniformity. It also provides a high plasma density and high dissociation of the gases [18], which may help achieve reasonable hardness.

We recently produced a-C:H coatings using the ECWR with a moderate wear-resistance, a wide optical gap of 3 eV and a low stress (<500 MPa) without damaging the plastic disks [19]. The films were deposited at near room temperature using methane as precursor. The ion energy was below 80 eV. Methane was used as a precursor in order to maximise the band gap, while maintaining a low heat load on the substrate. However, it was found during testing that these films were not hard enough to provide protection against damage during head crashes. Their density and Young's modulus are too low, at 1.2 g/cm^3 and 20 GPa, respectively. Indeed, it was found that contact atomic force microscopy could damage the coated disks. It became clear that the key problem is that the density was too low.

We have therefore carried out a further optimisation of growth conditions. The ECWR source was modified to increase the ion energy above 80 eV in order to improve the films' mechanical properties. A variety of hydrocarbon gas sources were used. Acetylene was used as a gas with less hydrogen in an effort to raise the film density, while propylene was used as representative of higher molecular weight gases which would have a higher growth rate than methane but without as high heat load. We now report wear-resistant, hard a-C:H coatings with a high transparency at 400 nm fit to protect the next generation of optical disks.

2. Experimental

The a-C:H films were grown on silicon, quartz and polycarbonate CD substrates using an ECWR plasma beam source of 14.2-in. diameter. This is much larger than the 6.6-in. source used in previous studies [18,20,21]. The source was modified to increase the ion energy above the previous limit of 80 eV. The new source configuration does not enable an independent electrical control of the ion energy and ion current. The ion energy is now decreased by increasing the pressure.

Methane, acetylene and propylene were used as precursor gases. Previous studies [21] using the smaller sources found that for C_2H_2 feed gas, the stress σ is relatively high: σ>5 GPa. In addition, the optical (Tauc) gap E_T was relatively low: E_T<2.1 eV. On the other hand, using CH_4 as precursor in the ECWR gives a lower stress, varying from 2.2 to 5 GPa depending on the ion energy [21]. The lower stress films have higher hydrogen content (between 50 and 32 at.% compared to 30% using C_2H_2) and smaller sp^3 fraction (0.58 compared to 0.75). For films using CH_4 as precursor, the optical gap was not reported [21]. No previous results were found for ECWR deposited films with propylene as precursor.

The ion energy was measured using a Faraday cup mounted in the substrate plane. Fig. 2A shows the evolution of the mean ion energy as a function of the pressure for an argon plasma (RF power: 800 W, distance between the cup and grid: 7.5 cm). It shows that the ion energy increases

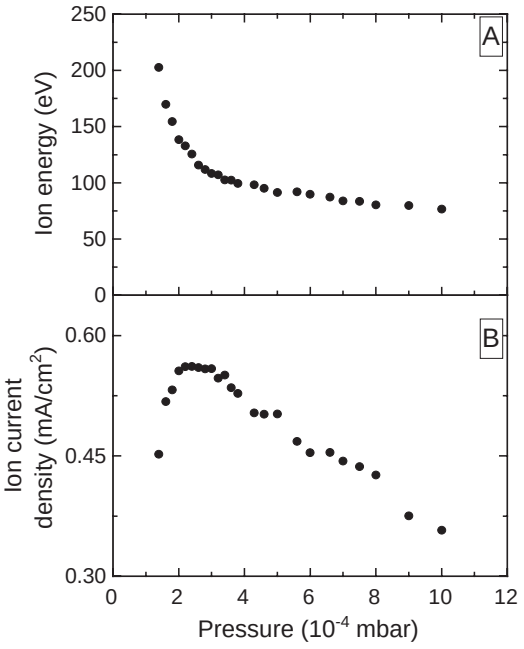

Fig. 2. Variation of (A) ion energy and (B) ion current density as a function of the pressure (Plasma: argon, RF power: 800 W, distance between the cup and grid: 7.5 cm).

when the pressure is decreased. It first increases slowly, from 98 to 76 eV when the pressure is decreased from 10^{-3} to 4.3×10^{-4} mbar. Then it increases rapidly with a further decrease of the pressure. It reaches 200 eV at 1.39×10^{-4} mbar. The trend observed in Ar plasma is expected to be similar in CH_4, C_2H_2 or C_3H_6 plasmas. Therefore, the ion energy can be varied significantly by decreasing the pressure.

The plasma pressure (P) and gas flow (F) were systematically varied for CH_4, C_2H_2 and C_3H_6 plasmas. The RF power and distance between the extraction grid and substrate were fixed at 600 W and 7 cm, respectively. The coil voltage and current were, respectively, 16 V and 1.1 A. The magnetic field strength B was of 13 G. The maximum temperature on the surface of the CD during deposition was estimated using commercially available temperature controller dots.

The films were characterized in terms of their structural, mechanical and optical properties. The film thickness and the refractive index at 633 nm were determined by ellipsometry using a Gaertner Scientific L117 ellipsometer. The optical properties were investigated by optical absorption spectroscopy using an ATI Unicam UV2-200 UV–Vis spectrophotometer over the 200–1100-nm wavelength range. For these measurements films were deposited on quartz, and both transmittance and reflectance spectra were recorded. The absorption coefficient was calculated and the E_{04} optical gap determined.

The stress was estimated from the Si substrate radius of curvature measured both before and after deposition using a Tencor Alpha-step 200 profilometer. A series of six measurements along two perpendicular directions in the middle of the sample were performed. The stress was then estimated using Stoney's equation. The Young's modulus E was measured by laser-induced surface acoustic waves (LISAW) [22].

The hydrogen content was determined from nuclear reaction analysis (NRA) using the resonance at 6.385 MeV of the reaction $^{15}N+^{1}H\rightarrow^{12}C+^{4}He+\gamma$. The effect of the hydrogen out-diffusion occurring during the bombardment with nitrogen ions was taken into account.

3. Results and discussion

3.1. Temperature of the disk surface and deposition rate

The temperature at the disk surface during deposition must be kept below 150 °C, the glass transition temperature of poly-carbonate. Fig. 3A shows the evolution of the maximum temperature at the CD surface during deposition, T_{MAX}, and Fig. 3B plots the deposition rate as a function of the plasma pressure for films deposited from the different gases. The deposition time was adjusted to keep a constant film thickness (~400 Å). Despite the dispersion of the data, Fig. 3A shows a general decrease of T_{MAX} with the pressure for all the precursor gases we used. The T_{MAX} value increases for lower pressures because of the rise in average ion energy and ion current seen in Fig. 2A and B.

The temperature rise is largest for methane, because its growth rate is so low. T_{MAX} exceeds 150 °C when $P\leq1.6\times10^{-3}$ mbar. Note that the maximum temperature that can be measured by the temperature dots is 154 °C.

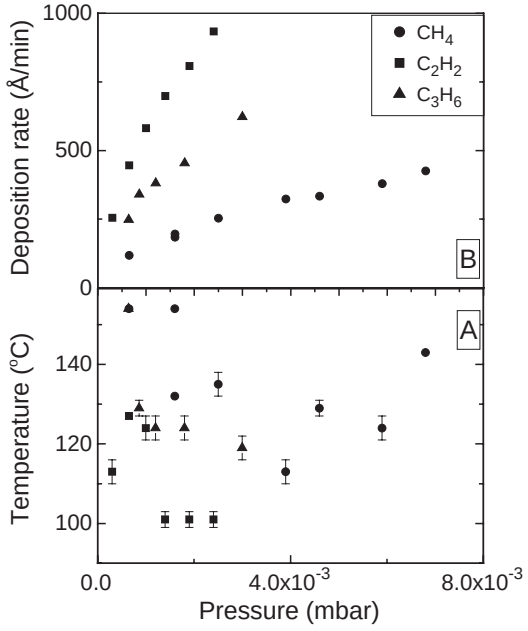

Fig. 3. (A) Maximum temperature at the surface of the CD during deposition for 400 Å thick films; (B) deposition rate as a function of the plasma pressure for films deposited from different precursors.

Consequently, T_{MAX} may be greater than 154 °C when $P \leq 1.6\times10^{-3}$ mbar. An increased production of hydrogen radicals at low pressure and their exothermic recombination at the surface could also contribute to T_{MAX}. Fig. 3 shows that, in order to preserve the CD integrity, CH_4 cannot be used as precursor when $P \leq 1.6\times10^{-3}$ mbar.

Fig. 3A indicates that T_{MAX} is much lower if C_2H_2 is used as precursor instead of CH_4. In the pressure range investigated, when C_2H_2 is used, $T_{MAX} \leq 130$ °C. Therefore, from a temperature point of view C_2H_2 can be used in the whole range of pressure investigated. The difference in T_{MAX} between C_2H_2 and CH_4 plasmas is due to the much higher deposition rate of C_2H_2 (Fig. 3B). At 6.5×10^{-4} mbar, the deposition rate is 3.8 times higher for C_2H_2. C_2H_2 plasmas also produce much less atomic hydrogen.

Noting that C_2H_2 gives rise to higher stress than CH_4, we also considered C_3H_6. We expect a higher deposition by using C_3H_6 instead of CH_4. We thus expect to grow films with less stress than with C_2H_2, but at the same time, we expect a lower T_{MAX}. Indeed, at 6.5×10^{-4} mbar, propylene gives a two times higher deposition rate than methane (Fig. 3B). However, T_{MAX} is still above 154 °C at $P=6.5\times10^{-4}$ mbar for C_3H_6. T_{MAX} then decreases rapidly with the pressure (Fig. 3A) so that from a temperature point of view, it is possible to use C_3H_6 as precursor for $P > 6.5\times10^{-4}$ mbar.

For each precursor, the deposition rate increases rapidly with the pressure. The increase is greatest for C_2H_2. In this case, the deposition rate increases from 255 to 934 Å/min when the pressure is increased from 3×10^{-4} to 2.4×10^{-4} mbar. However, at the highest pressures, the high growth rates with C_2H_2 degrade the adhesion on quartz and films could no longer be measured.

3.2. Optical band gap and stress

Fig. 4 shows the evolution of the hydrogen content (A), stress (B), and the E_{04} optical gap (C) as a function of the plasma pressure for films deposited from different precursors. We note that the optical absorption edge of a-C:H is broad, so that in fact the optical absorption coefficient at 400 nm is the actual required parameter. However, the ratio of the slope of the edge, the Urbach energy and the optical gap is roughly constant for the a-C:H of interest [10,23]; therefore, the optimisation can be characterised in terms of a single parameter, the gap. Fig. 4C shows that E_{04} exceeds 3 eV for all precursors, if T_{MAX} is also not exceeded (see Section 3.1). The values obtained with C_2H_2 as precursor are higher than those previously reported using it and the 6-in. ECWR source [21].

Fig. 4B shows that the stress varies significantly with the precursor used. In the case of C_2H_2, the stress is high. It decreases from ~6.5 to 4.6 GPa when the pressure is increased from 3×10^{-4} to 2.4×10^{-4} mbar. However, these are still very high values and illustrate why methane was used previously [19]. The stress is expected to decrease with

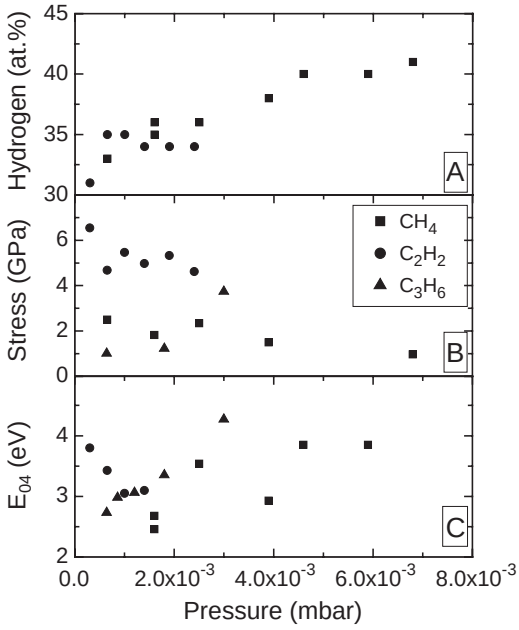

Fig. 4. (A) Hydrogen content, (B) stress, and (C) E_{04} optical gap as a function of the plasma pressure for films deposited from different precursors.

increasing pressure because of the decrease of average ion energy in Fig. 2A. When CH_4 or C_3H_6 are used as precursors, the stress is lower. For CH_4 the stress decreases from ~2.5 to 1 GPa when the pressure is increased from 6.5×10^{-4} to 6.8×10^{-3} mbar. For C_3H_6 the evolution of the stress with the pressure is less clear. The stress reaches 3.7 GPa at 3×10^{-3} mbar.

Even though the stress is still relatively high, no buckling, cracks or blur effects were observed on the coatings deposited onto disks. However, the high stress bends the disk. The deflection is higher than the specification of 50 μm, the maximum acceptable for CDs [4]. In fact, we estimated by using Stoney's equation that to obtain a deflexion less than 50 μm on poly-carbonate, the stress must be lower than ~250 MPa. This is much less than the stress values commonly reported for wear-resistant DLC films (≥2 GPa). In order to reduce the deflexion of the CDs induced by the DLC, both sides of the CDs have been coated with the same DLC layer. In this case, the resulting deflexion is below 50 μm, even when both sides of the CD are coated with a high-stress DLC layer (5 GPa) deposited using C_2H_2 as precursor at $P=1.4\times10^{-3}$ mbar.

3.3. Refractive index, density, and Young's modulus

Fig. 5 shows the evolution of the Young's modulus, E (A), density, ρ (B), and refractive index, n (C), measured at 633 nm as a function of the plasma pressure for films deposited from C_2H_2 or CH_4. Fig. 5 shows that the films obtained from CH_4, have a low density ($1.2 \leq \rho \leq 1.4$ g/cm^3), refractive index ($1.75 \leq n \leq 1.96$), and Young's modulus (E=20 GPa). These values are too low and are similar to

the previous films [19]. These films are not hard enough to provide protection against damage during head crashes. This eliminates methane as a possible precursor.

The best precursor for mechanical properties is C_2H_2 (Fig. 5). This is because its films have the highest density for a given pressure and thus, the highest modulus. At P=1.4×10^{-3} mbar, the films from C_2H_2 have a higher refractive index (n=2.12), density (ρ~1.8 g/cm^3), and Young's modulus (E~120 GPa). The films produced in these conditions are hard enough to protect the CDs during head crashes. However, they have high stress (Section 3.2). It is thus necessary to coat both sides of CDs to reduce the curvature of the CDs induced by stress (Section 3.2).

The relatively low values of the Young's modulus obtained here compared to previous films produced by the small ECWR [24] can be explained by the relatively high incorporation of hydrogen (Fig. 4A). This happens even when C_2H_2 is used as precursor because of the much higher plasma pressure used here, compared to the standard, much lower pressure conditions used to produce tetrahedral amorphous carbon (ta-C:H) [18,20]. The higher H content is due to the high gas pressure here [18].

For a-C:H films it is possible to use the refractive index at 633 nm as a rapid means of estimating the mechanical properties [25]. Fig. 6 shows the evolution of refractive index (A) and Young's modulus (B) as a function of density for films deposited by different techniques, including RF-PECVD, a 6-in. ECWR plasma beam source, an ECR plasma from different hydrocarbon source gases [26], and a DECR C_2H_2 plasma [16,27,28]. Despite some scatter of the data, Fig. 6A shows that the mass density increases with the refractive index. Fig. 6B shows that Young's modulus increases with the density, in a similar way to that found for

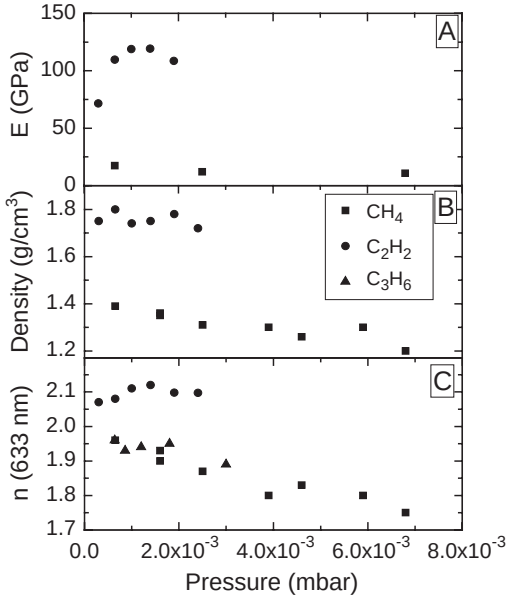

Fig. 5. (A) Young's modulus, (B) density, and (C) refractive index at 633 nm as a function of the plasma pressure for films deposited from different precursors.

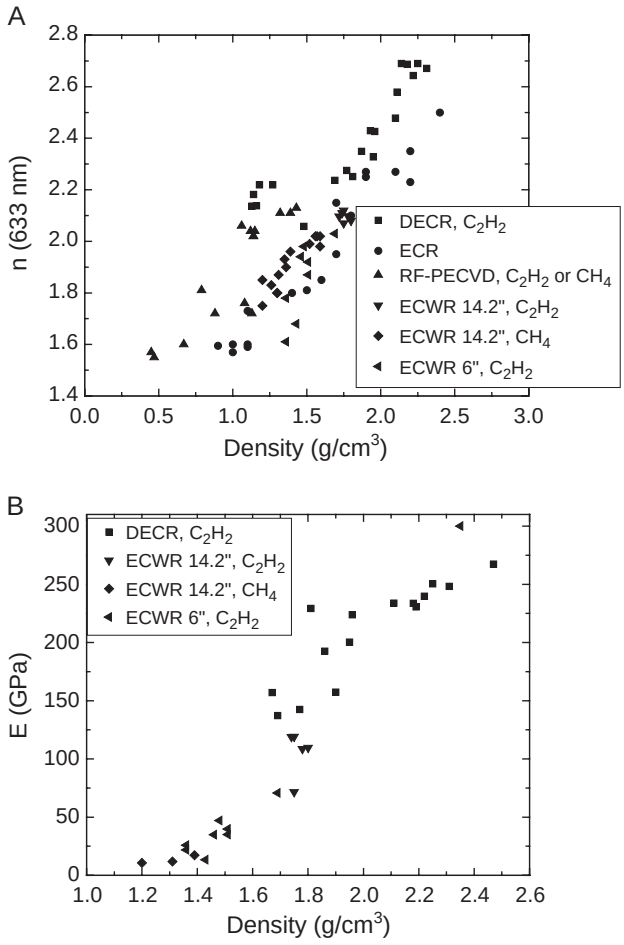

Fig. 6. (A) Refractive index as a function of density for films deposited by different techniques and from different precursors: (■) DECR plasma from C_2H_2 [16,27]; (●) ECR from different hydrocarbon source gases [26]; (▲) RF-PECVD system from C_2H_2 and CH_4; (▼) 14.2-in. ECWR plasma beam source from C_2H_2; (♦) from CH_4; (◄) 6-in. ECWR plasma beam source from C_2H_2; (B) Young's modulus as a function of density for films deposited by different techniques: (■) DECR plasma from C_2H_2 [16,27,28]; (▼)14.2-in. ECWR plasma beam source from C_2H_2; (♦) from CH_4; (◄) 6-in. ECWR plasma beam source from C_2H_2.

H-free carbons [24]. This can be understood in that the modulus depends on the fraction of C–C sp^3 bonds, and the density depends on the C concentration, as H is so light.

4. Conclusions

We reported the deposition of large area hydrogenated amorphous carbon films for next generation ultra-high storage density optical disks. The films deposited at 1.4×10^{-3} mbar from C_2H_2 as precursor show a suitable wear-resistance, an optical gap of 3.1 eV, mass density of ~1.8 g/cm^3, and Young's modulus of ~120 GPa. The stress is high (5 GPa), but the deflection of the CD is lower than 50 μm if both sides of the CD are coated with the same layer. The films are deposited at a high rate (700 Å/min), with less than 9% thickness variation over 12 cm and

negligible structural variations. The maximum temperature at the surface of the CD during deposition is of 100 °C.

Acknowledgements

The authors would like to thank Arburg for providing the CDs used in this work. The work was supported by the European Community (FAMOUS; Project IST-2000-28661). ACF acknowledged funding from The Royal Society.

References

[1] J. Hellmig, Phys. World 17 (2004) 21.
[2] H. Awano, N. Ohta, IEEE J. Sel. Top. Quantum Electron. 4 (1998) 815.
[3] T. Sakamoto, G. Fujita, A. Nakaoki, J. Mag. Soc. Jap. 25 (2001) 1261.
[4] C. Morsbach, C. Dubarry, M. Gabriel, M. Hoyer, S. Knappmann, F. Piazza, J. Robertson, R. Vullers, H.H. Gatzen, IEE Proc. Sci. Meas. Technol. 150 (2003) 203.
[5] M.F. Doerner, R.L. White, Mat. Res. Symp. Bull. 28 (1996).
[6] B. Bhushan, Diamond Relat. Mater. 8 (1999) 1985.
[7] J. Robertson, Thin Solid Films 383 (2001) 81;
A.C. Ferrari, Surf. Coat. Technol. 180 (2004) 190.
[8] P. Goglia, J. Berkowitz, J. Hoehn, A. Xidis, L. Stover, Diamond Relat. Mater. 10 (2001) 271.
[9] C. Casiraghi, A.C. Ferrari, D.P. Chu, A.J. Flewitt, J. Robertson, Phys. Rev. Lett. 91 (2003) 226104.
[10] J. Robertson, Mater. Sci. Eng. R 37 (2002) 129;
Adv. Phys. 35 (1986) 317.
[11] M. Weiler, S. Sattel, T. Giessen, K. Jung, H. Ehrhardt, V.S. Veerasamy, J. Robertson, Phys. Rev. B 53 (1996) 1594.
[12] M.A. Tamor, W.C. Vassell, J. Appl. Phys. 76 (1994) 3823.
[13] A.C. Ferrari, S.E. Rodil, J. Robertson, W.I. Milne, Diamond Relat. Mater. 11 (2002) 994.
[14] A.C. Ferrari, J. Robertson, Phys. Rev. B 61 (2000) 14095.
[15] C.H. Lee, W.R.L. Lambrecht, B. Segall, P.C. Kelires, T. Frauenheim, U. Stephan, Phys. Rev. B 49 (1994) 11448.
[16] A. Golanski, F. Piazza, J. Werckmann, G. Relihan, S. Schulze, J. Appl. Phys. 92 (2002) 3662.
[17] A. Golanski, J.P. Stoquert, P. Kern, F. Piazza, S. Schulze, Nucl. Instrum. Methods B 206 (2003) 731.
[18] M. Weiler, K. Lang, E. Li, J. Robertson, Appl. Phys. 72 (1998) 1314.
[19] F. Piazza, D. Grambole, L. Zhou, F. Talke, C. Casiraghi, A.C. Ferrari, J. Robertson, Diamond Relat. Mater. 13 (2004) 1505.
[20] N.A. Morrison, S.E. Rodil, A.C. Ferrari, J. Robertson, W.I. Milne, Thin Solid Films 337 (1999) 71.
[21] N.A. Morrison, C. Williams, B. Racine, W.I. Milne, E. Martinez, J. Esteve, J.L. Andujar, Curr. Appl. Phys. 3 (2003) 433.
[22] D. Schneider, T. Schwartz, H.J. Scheibe, M. Panzner, Thin Solid Films 295 (1997) 107.
[23] G. Fanchini, A. Tagliaferro, Appl. Phys. Lett. 85 (2004) 730.
[24] A.C. Ferrari, J. Robertson, M.G. Beghi, C.E. Bottani, R. Ferulano, R. Pastorelli, Appl. Phys. Lett. 75 (1999) 1893.
[25] C. Casiraghi, F. Piazza, A.C. Ferrari, D. Grambole, J. Robertson, Diamond Relat. Mater., in press.
[26] T. Schwarz-Sellinger, A. von Keudell, W. Jacob, J. Appl. Phys. 86 (1999) 3988.
[27] F. Piazza, G. Golanski, S. Schulze, G. Relihan, Appl. Phys. Lett. 82 (2003) 358.
[28] F. Piazza, Int. J. Ref. Metals & Hard Mater. (submitted for publication).